Electronic properties of $3R$-$CuAlO_2$ under pressure: Three theoretical approaches

N. E. Christensen,[1] A. Svane,[1] R. Laskowski,[2] B. Palanivel,[3] P. Modak,[4] A. N. Chantis,[5] M. van Schilfgaarde,[6] and T. Kotani[7]

[1]*Department of Physics and Astronomy, Aarhus University, DK-8000 Aarhus C, Denmark*
[2]*Institute of Materials Chemistry, Technical University of Vienna, Getreidemarkt 9/165TC, A-1060 Vienna, Austria*
[3]*Department of Physics, Pondicherry Engineering College, Puducherry 605 014, India*
[4]*High Pressure Physics Division, Bhabha Atomic Research Centre, Trombay, Mumbai 400085, India*
[5]*Theoretical Division, Los Alamos National Laboratory, Los Alamos, New Mexico 87545, USA*
[6]*School of Materials, Arizona State University, Tempe, Arizona 85287-6006, USA*
[7]*Department of Applied Physics and Mathematics, Tottori University, Tottori 680-8552, Japan*

(Received 7 August 2009; revised manuscript received 6 October 2009; published 14 January 2010)

The pressure variation in the structural parameters, u and c/a, of the delafossite $CuAlO_2$ is calculated within the local-density approximation (LDA). Further, the electronic structures as obtained by different approximations are compared: LDA, LDA+U, and a recently developed "quasiparticle self-consistent GW"(QSGW) approximation. The structural parameters obtained by the LDA agree very well with experiments but, as expected, gaps in the formal band structure are underestimated as compared to optical experiments. The (in LDA too high lying) Cu $3d$ states can be down shifted by LDA+U. The magnitude of the electric field gradient (EFG) as obtained within the LDA is far too small. It can be "fitted" to experiments in LDA+U but a simultaneous adjustment of the EFG and the gap cannot be obtained with a single U value. QSGW yields reasonable values for both quantities. LDA and QSGW yield significantly different values for some of the band-gap deformation potentials but calculations within both approximations predict that $3R$-$CuAlO_2$ remains an indirect-gap semiconductor at all pressures in its stability range 0–36 GPa, although the smallest direct gap has a negative pressure coefficient.

DOI: 10.1103/PhysRevB.81.045203 PACS number(s): 71.15.Qe, 71.35.Cc, 78.20.Ci, 78.40.Fy

I. INTRODUCTION

Copper aluminate, $CuAlO_2$, belongs to a large class of minerals called *delafossites*, referring to a specific member of the family, $CuFeO_2$. It was first studied in 1872 by Friedel,[1] who named it after the French crystallographer Gabriel Delafosse. Copper aluminate is of particular technological interest because it, without intentional doping, is a p-type conducting, transparent oxide.[2,3] Usually optically transparent oxides are electrical insulators due to their large gap but a few exceptions, such as SnO_2 and In_2O_3 are known. However, these are (doped) n-type conductors. Transparent, conducting oxides are used in flat panel displays. The availability of p-type material opens for new "functionalities" involving p-n junctions. Also, introducing magnetic impurities in $CuAlO_2$, new diluted magnetic semiconductors can be produced.[4,5] It has also been demonstrated[6,7] that $CuAlO_2$ may become a good thermoelectric material with promising future applications.

The modification "$R3$" of $CuAlO_2$ crystallizes in a structure which belongs to the space group $R\bar{3}m$ or $P6_3/mmc$. It can be viewed as a layered hexagonal structure, see Fig. 1. The figure shows the trimolecular hexagonal cell. In the present calculations the structure was built of primitive (1 f.u.) rhombohedral cells, with the atoms placed at the Wyckoff positions: Cu: (1a) (0,0,0), Al: (1b) (1/2,1/2,1/2), and O: (2c) $\pm(u,u,u)$. Using $a_r=a/\sqrt{3}$ as a length unit, the rhombohedral primitive translations are: $[1,0,c_r/(\sqrt{3}a_r)]$, $[-1/2,\sqrt{3}/2,c_r/(\sqrt{3}a_r)]$, and $[-1/2,-\sqrt{3}/2,c_r/(\sqrt{3}a_r)]$. Here $c_r=c/\sqrt{3}$ and $c_r/a_r=c/a$.

The Cu cations are linearly coordinated by O and the CuO_2 dumbbells are separated by a layer of edge sharing MO_6 octahedra. Kawazoe *et al.*[3] proposed that the monopolarity in these compounds results from localization of the holes at the oxygen $2p$ levels due to the strong electronegativity of the oxygen atoms. Since the energies of the Cu $3d$ orbitals are quite close to the O $2p$ states the strong covalent bonding between Cu and O delocalizes the positive holes.[3,8] Further, the low Cu-O coordination leads to a weaker interaction and thus to a larger band gap when compared to Cu_2O, for example. The direct and indirect band gaps of $CuAlO_2$ were estimated as about 3.5 and 1.8 eV.[3,8] Several x-ray spectroscopy studies indicate that both, the valence and conduction bands result from strong mixing of Cu $3d$ and O $2p$ states.[8,9] A detailed study of the electronic structure of $CuAlO_2$ has been performed by Aston *et al.*[9] using x-ray photoemission spectroscopy (XPS), x-ray emission spectroscopy, and x-ray absorption spectroscopy. According to their findings the maximum of the Cu $3d$ band appears about 2.8 eV below the valence-band maximum (VBM) and the maximum of the O $2p$ band is located around 5 eV below the VBM. They also found a relatively good agreement with *ab initio* calculations. However the calculated Cu $3d$ band is too close to the VBM, its binding energy being only $\approx$1.2 eV. The calculated band structure shows a dispersion of the valence bands around the F and L points in the Brillouin zone (BZ) (see Ref. 10) mainly due to the interaction between Cu d_{z^2} and O p_z states,[11] whereas relatively flat bands (see Fig. 4 in Ref. 11) around Γ and Z originate from antibonding Cu-O π states. The series of $CuMO_2$ delafossites, where M is Al, Ga, or In shows band-gap anomalies. The *optically* measured gaps are 3.5 eV for $CuAlO_2$, 3.6 eV for $CuGaO_2$, and 3.9 for $CuInO_2$. This trend contradicts observed trends

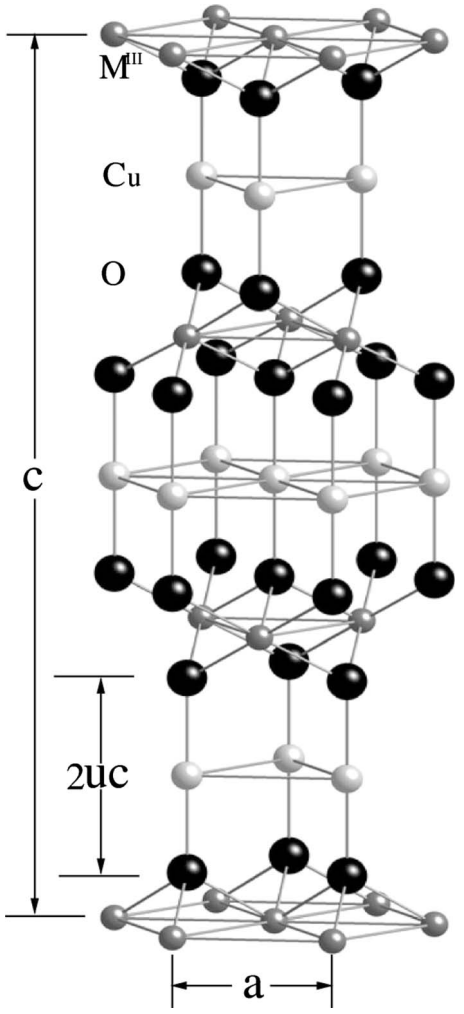

FIG. 1. The structure of 3*R*-$CuAlO_2$ (M^{III}=Al). The figure shows the trimolecular hexagonal cell.

for other group-III containing semiconductors. Using a first-principles method, based on the local-density approximation (LDA) to the density-functional theory, Nie *et al.*[12] gave a simple explanation of this anomaly. They found that the direct gaps follow the general trend and decrease within the series. However, the region of the BZ around Γ is optically inactive. It happens that for $CuInO_2$ and $CuGaO_2$ the fundamental gaps are at Γ, whereas the optically allowed transitions start at higher energies around L.

The theory of optical absorption in $CuAlO_2$, applying a combination of LDA+U (Refs. 13–15) [Coulomb-interaction (U) corrected LDA] and solution of the Bethe-Salpeter equation (BSE) (Ref. 16) was presented earlier.[17] The present work aims at a comparison of LDA, LDA+U, and quasiparticle band-structure calculations. The latter relates to optical properties but does not include the effects of electron-hole (e-h) correlations (which were treated in the BSE calculations). The quasiparticle bands are calculated by means of the "quasiparticle self-consistent *GW*" (QS*GW*) approximation by van Schilfgaarde *et al.*[18–21] (G: Green's function and W: screened Coulomb interaction).

The paper is organized as follows. Section II describes the calculations (LDA) of structural parameters, pressure, and bulk modulus vs volume, and comparison to experimental results. In Sec. III the LDA, LDA+U and QS*GW* bands are compared and in Sec. IVthe deformation potentials and pressure coefficients as derived from LDA and QS*GW* calculations are discussed. In Sec. V we discuss the spectral position of the Cu 3*d* states and its influence on the Cu electric field gradient (EFG). Summary and conclusions follow in the last Sec. VI.

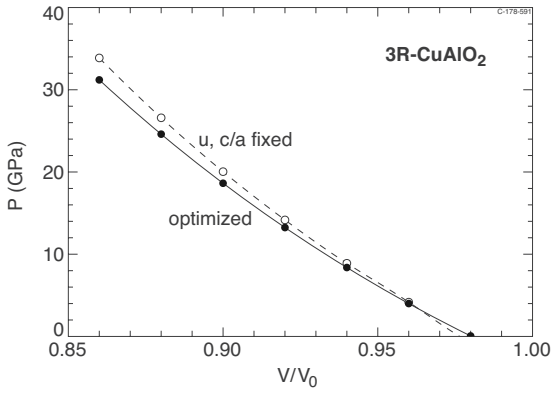

FIG. 2. Pressure-volume relations calculated with and without optimization of c/a and u. V_0 is the experimental equilibrium volume. The theoretical LDA equilibrium volume is $0.98V_0$, where the pressure is zero (optimized structural parameters).

II. STRUCTURAL PARAMETERS (LDA)

LDA calculations of structural parameters and some including phonon frequencies have been published earlier for some delafossites, see, for example, Refs. 12 and 22–24, and references therein. Theoretical variations in the structural parameters with volume were presented in Ref. 25 but experimental results have only been published for ambient pressure. In the present work the parameters, c/a and u, (see Fig. 1) were optimized for volumes, V, ranging from the experimental equilibrium ($V=V_0$) down to $0.86\times V_0$. Our c/a values are somewhat smaller than those calculated in Ref. 25. The total-energy minimization, derivation of the pressure, P, and bulk modulus, B, were performed by means of the linear muffin-tin orbital method (LMTO) (Ref. 26) in a full-potential version.

Volumes are related to the experimental equilibrium value, V_0, for which a is 2.858 Å, c is 16.958 Å, and u =0.1099 (as quoted in Refs. 12 and 27). Figure 2 shows two calculated P-V relations, one where the internal parameters were fixed to their experimental equilibrium values and another where c/a and u were optimized at each volume. In both cases the theoretical equilibrium volume is ≈2% smaller than V_0. In view of the tendency to overbinding in the LDA and the fact that we omit thermal effects and zero-point phonon contributions, the agreement between theory and experiment is satisfactory. Also the volume variation in the bulk modulus, B, was calculated with and without optimization of c/a and u, see Fig. 3. The effect of the structural optimization is more pronounced in this case than for P-V, which can be expected since B is related to the second volume derivative of the total energy, whereas P only involves

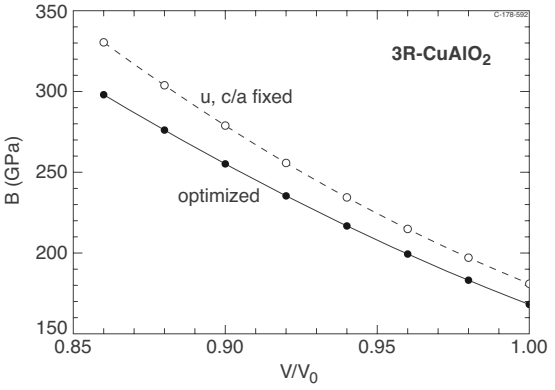

FIG. 3. Bulk modulus vs volume calculated with and without optimization of c/a, uV_0 is the experimental equilibrium volume, and the theoretical zero-pressure volume is $0.98V_0$.

the first-order derivative. The values at V_0, $B \approx 170$ (u and c/a optimized) and 180 GPa (u and c/a fixed to the experimental values) are smaller than the experimental value 200 ± 10 GPa obtained by Pellicer-Porres *et al.*[24] Our *theoretical* (LDA) value of B is 180 GPa, evaluated at the theoretical equilibrium volume with optimized c/a and u parameters.

The volume variation in the internal parameters, c/a and u, is illustrated in Fig. 4. Since we only have access to experimental values of c/a and u at $V=V_0$, we can only compare our calculated parameters to measured data for that volume. Excellent agreement is obtained, see caption of Fig. 4.

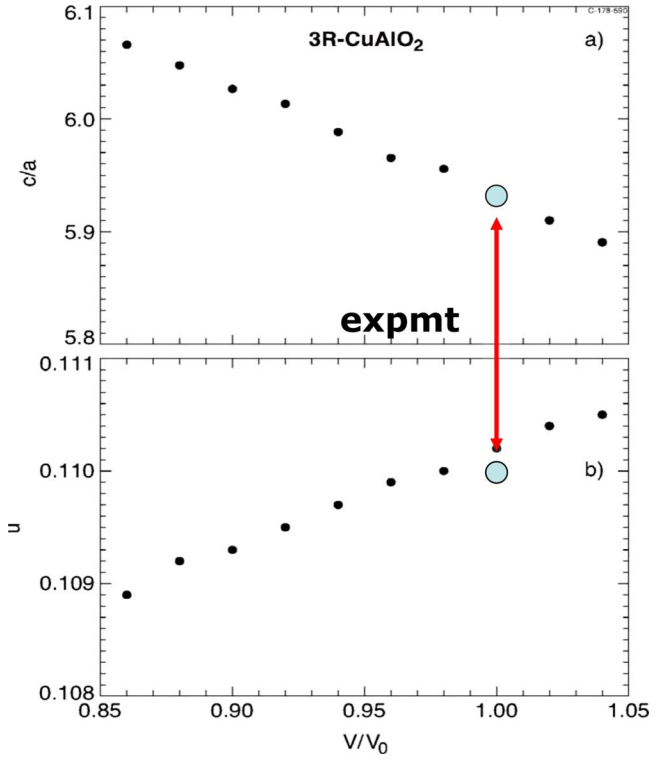

FIG. 4. (Color online) (a) axial ratio, c/a and (b) internal parameter, u, vs volume. The experimental values, quoted in Ref. 27, are $c/a=5.9335$ and $u=0.1099$ at equilibrium, whereas the calculated values are 5.9331 and 0.1102, also for $V=V_0$ (the experimental equilibrium volume).

As might be expected, the standard LDA combined with a "state-of-the-art" band-structure method performs well for prediction of the ground-state properties (structure) of a material such as copper aluminate, presumably without particularly strong correlation effects. However, as will be shown later, this does not necessarily mean that all ground-state properties of this material can be predicted by LDA. And in fact, an improper description of the Cu d states could affect the calculated equilibrium volume. The "LDA error" in positioning the $3d$ states in energy in Zn containing II-VI semiconductors is not negligible and in pure Zn it leads to an 11% overbinding (Fig. 34 of Ref. 28).

III. LDA, LDA+U, AND QSGW BAND STRUCTURES

At the end of the previous section it was mentioned that the LDA to the density-functional theory may treat some states, like the d states in materials containing $3d$ transition metals, as well as some semicore states, incorrectly. Too high energies of these states imply that their hybridization with (other) valence states is overestimated and the LDA overbinding is further increased. For $CuAlO_2$ we examine this problem by means of LDA+U calculations. Some effects of LDA+U on ground-state properties will be discussed in the next section.

The formal one-electron energies in the Kohn-Sham equation are, in principle, not well suited for analyses of optical experiments. However, the LDA band structures have in numerous cases been very useful also for such purposes, for semiconductors often after *ad hoc* corrections[29,30] for the severely underestimated band gaps. From a theoretical point of view more well founded methods for calculating quasiparticle band structures which can be related to optical properties should be applied.

First, since LDA+U will generate a downshift of the Cu $3d$ states, it was examined to which extent the reduction in hybridization with the uppermost valence-band states can increase the gap in $CuAlO_2$ to match optical experiments. This was used in Ref. 17, where the downshift was produced by adding an orbital potential, V^{FLL}, which in the formally "fully localized limit" as introduced by Anisimov *et al.*[14] has the form

$$V^{FLL} = (U - J)\left(\frac{1}{2} - \hat{n}_\sigma\right), \tag{1}$$

where $\hat{n}_\sigma$ gives the occupancy of the orbital σ. In order to avoid double counting in the nonspherical part of the potential, an effective Hubbard U, $U_{eff}=U-J$ is used instead of separate U and J, and also the multipolar term proportional to J in the LDA+U potential is omitted. Since the occupancies of all the Cu $3d$ orbitals are larger than 1/2, the potential V^{FLL} shifts the center of "gravity" of the d states towards lower energies. The shift is proportional to the value of U_{eff}. The operator $\hat{n}_\sigma$ projects out the occupancy of the orbital σ. For a fully occupied state it gives 1 and for an empty state 0, thus a full state is downshifted by $U_{eff}/2$. However, the d orbitals in the solid (the Cu $3d$ here) have occupation fractions which are somewhat less than 1 due to hybridization

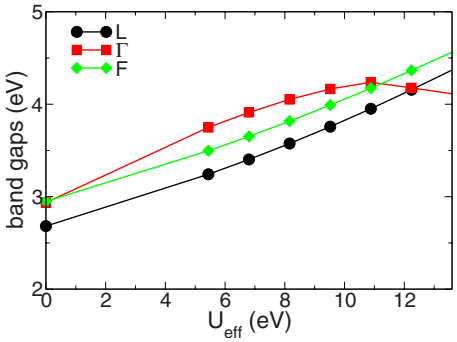

FIG. 5. (Color online) LDA+U: Direct gaps at L, Γ, and F as functions of U_{eff}.

and therefore the 3d states will be downshifted by an amount smaller than $U_{eff}/2$.

It was found that a choice of U_{eff}=8.2 eV produces a down shift of the Cu 3d peak in the density of states (DOS) so that agreement is obtained with the XPS data obtained by Aston *et al.*[9] Simultaneously, the lowest direct gap (at the L point) has opened (see Fig. 5) to ≈3.5 eV, i.e. also as found experimentally.[23] This is also seen clearly in Fig. 6, where the LDA and LDA+U band structures are compared. The inclusion of the U corrections lowers the position of the Cu 3d bands and reduces their width.

Although it is possible, by choosing a proper value of U_{eff}, by means of LDA+U to obtain a band structure which is considerably better as basis for description of optical properties than the pure LDA bands, it is desirable to apply a parameter-free method to obtain a theoretical quasiparticle band structure for such purposes. As "input" to calculations of optical properties, for example, solving the BSE, we need a good quasiparticle band structure. The GW is one such scheme.[31] The GW approximation can be viewed as the first term in the expansion of the nonlocal energy-dependent self-energy $\Sigma(\mathbf{r},\mathbf{r}',\omega)$ in the screened Coulomb interaction W. From a more physical point of view it can be interpreted as a dynamically screened Hartree-Fock approximation plus a Coulomb hole contribution.[31] It is also a prescription for mapping the noninteracting Green's function to the dressed one, $G^0 \rightarrow G$. In the QSGW scheme a prescription is given on

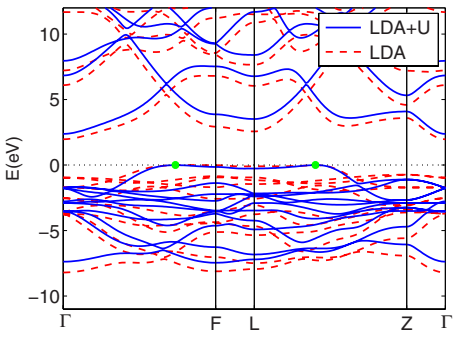

FIG. 6. (Color online) Band structures for 3R-$CuAlO_2$ LDA (red, dashed lines) and LDA+U with U_{eff}=8.2 eV (blue, full-line curves). The energy was set to zero at the VBM, indicated by the two dots (green). The bands are shown along lines, which were selected consistently with the choice in Ref. 8.

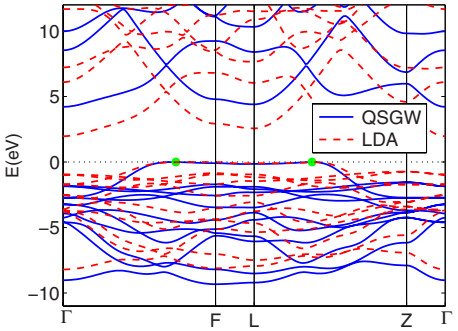

FIG. 7. (Color online) Band structures for 3R-$CuAlO_2$ LDA (red, dashed lines) and QSGW (blue, full-line curves). The energy was set to zero at the VBM, indicated by the dot at a point on the Γ-F line. See also the note Ref. 37.

how to map G to a new noninteracting Green's function $G \rightarrow G^0$. This is used for the input to a new iteration. The procedure is repeated $G^0 \rightarrow G \rightarrow G^0 \rightarrow \cdots$ until convergence is reached. Thus QSGW is a self-consistent perturbation theory, where the self-consistency minimizes the magnitude of the perturbation. The QSGW is parameter free, independent of basis set and of the LDA. Details of this scheme can be found in Refs. 19 and 20. It has been shown that QSGW reliably describes the band structure in a wide range of materials.[18,21,32–35] The QSGW approximation in the current implementation uses the full-potential LMTO method.[26,36]

In Fig. 7 we compare the band structures calculated within the LDA and the QSGW schemes. In both cases the minimum direct gap is found at the L point. (Note that our choice of symmetry lines is different from that in Ref. 11 referred to in Sec. I). The valence-band maximum is not at F but rather[37] at the point marked with a dot at a point on the Γ-F line, where the energy is 0.084 eV (QSGW) above the highest valence-state energy at F. The maximum along L-Z is 0.3 meV below the VBM. The gaps in the QSGW band are substantially larger than those obtained with the LDA. The values of the gaps at the four high-symmetry points, Γ, F, L, and Z are 2.90, 2.93, 2.66, and 4.28 with LDA, whereas the QSGW values are 5.99, 4.87, 4.55, and 7.47 eV, respectively. The smallest direct QSGW gap, 4.55 eV, is 1 eV larger than what has been measured. A systematic overestimate of the gaps in semiconductors as derived by the QSGW is normal[18] and is partly due to the omission of vertex corrections. The e-h correlations are part of this and they can give rise to significant corrections to the gaps. Shishkin *et al.*[38] calculated the e-h gap reductions ($\Delta_{e\text{-}h}$) for a number of semiconductors (not $CuAlO_2$) and, in general, they are on the order of some tenths of an electron volt, 0.23 eV for GaAs, and very large, 1.04 eV, for MgO, where the gap itself is large (7.8 eV). We have made a rough estimate of $\Delta_{e\text{-}h}$ for $CuAlO_2$ from our BSE calculations[17] by determining the downshift in energy of spectral features in the dielectric functions as derived from the input quasiparticle bands and as seen in the BSE spectrum. For polarization parallel to the c axis we get $\Delta_{e\text{-}h} \approx 0.8$ eV. For perpendicular polarization the estimate is more uncertain since the lower part of the BSE spectrum[17] is not clearly separated from the somewhat broadened exciton states in the gap. In order to evaluate our method of estimat-

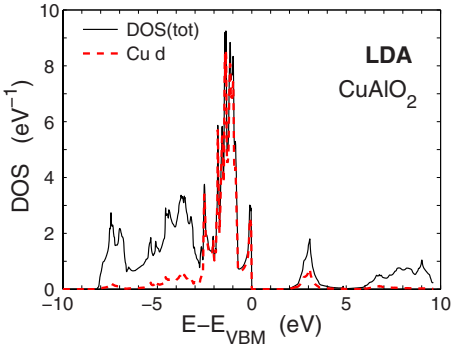

FIG. 8. (Color online) 3*R*-$CuAlO_2$ LDA: DOS functions. Only Cu 3*d* and total DOS functions are shown. E_{VBM} is the energy at the valence-band maximum.

ing $\Delta_{e\text{-}h}$ we applied the same method to other semiconductors. For AlN we get $\Delta_{e\text{-}h} \approx 0.8$ eV (using the BSE calculations in Ref. 39), ZnO: 0.7 eV (BSE: Ref. 40), and GaN: 0.6 eV (BSE: Ref. 41). The values extracted from Table 1 of Ref. 38 are for ZnO: 0.6 eV and for GaN: 0.55 eV, respectively. These are close to our estimates and we therefore believe that also the value obtained here for the e-h gap reduction in $CuAlO_2$ is reasonable.

The comparison of theoretical and experimental band gaps is further complicated by the fact that electron-phonon interactions renormalize the gaps. Such effects are not included in our calculations. Often the experiments are carried out at ambient temperature (T), where the gaps are smaller than near $T=0$. The generally accepted value of the gap in GaAs at $T=300$ K is 1.42 eV, whereas the value at very low T is 1.52 eV. Thus corrections on the order of one or a few tenths of an electron volt can be expected. In cases where careful measurements of the gap (E_g) vs T, ranging down to very low temperatures are not available, it is usual to apply extrapolations. Frequently these are made by means of the empirical law for $E_g(T)$ proposed by Varshni,[42]

$$E_g(T) = E_0 - \frac{\alpha T^2}{T+\beta}, \tag{2}$$

where α and β are adjustable parameters. At high temperatures the relation is essentially linear. At low T it exhibits an asymtotic T^2 behavior. This T dependence is not correct as

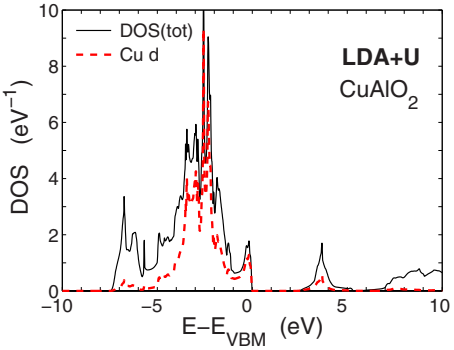

FIG. 9. (Color online) 3*R*-$CuAlO_2$ LDA+*U*: density of states functions, total and Cu 3*d* partial DOS.

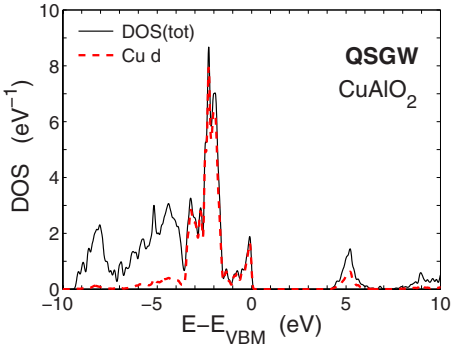

FIG. 10. (Color online) 3*R*-$CuAlO_2$ QS*GW*: density of states functions, total and Cu 3*d* partial DOS.

demonstrated by Cardona *et al.*[43,44] Rather, a T^4 asymptotic behavior is found (using a Debye phonon model). It was also shown that the zero-point lattice vibrations can contribute essentially to the gap renormalization. Gap changes due to thermal lattice expansion/contraction are usually small on the energy scale relevant here.

Therefore, the fact that the QS*GW* approximation systematically overestimates the gaps in semiconductors, as found here and in many other calculations, does not invalidate the approach since there are obvious corrections which should be included in order to obtain higher accuracy when the results are compared to experiments. The fact that we here find a gap which is ≈ 1 eV too large may still be explainable by these known effects.

IV. Cu 3*d*-BAND POSITION AND Cu EFG

The band structures in Fig. 7 show that the QS*GW* has shifted the Cu *d* states down relative to the VBM. This is more clearly seen by comparing the DOS functions as derived by LDA, LDA+*U*, and QS*GW*, Figs. 8–10. In addition, we compare in Fig. 11 the Cu *d* DOS obtained within the three approximations. The LDA+*U* *d* DOS is lowest in energy and its shape differs clearly from those of the LDA and QS*GW* *d* DOS. However, this difference can be reduced by choosing a smaller value of U_{eff}.

The downshift produced by LDA+*U* and QS*GW* is similar to the effect which we wanted to simulate by the simple

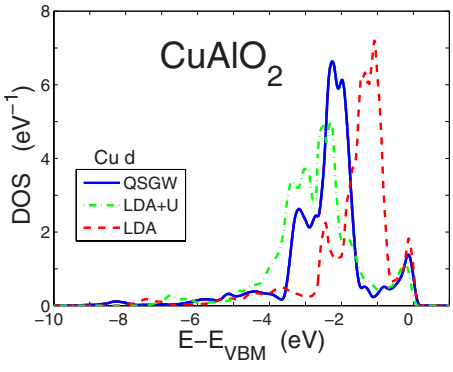

FIG. 11. (Color online) 3*R*-$CuAlO_2$: Cu 3*d* density-of-states functions (smoothed) as calculated by the three approximations: LDA, LDA+*U* ($U_{eff}=8.2$ eV), and QS*GW*.

procedure,[28] see also Fig. 11 in Ref. 45, where the Zn $3d$ states were shifted down by ≈ 2 eV in each iteration by redefining the band-center potential parameter in the LMTO.[26] The same scheme was applied to the $4d$ states of tin in order to improve the α- β-tin total-energy difference.[46] The down shift reflects the correlation corrections to ground-state properties as predicted from the LDA.

Atomic nuclei with spin I larger than 1/2 have quadrupole moments. ^{63}Cu has $I=3/2$ and it is then such a case. Nuclear quadrupole resonance (NQR) measures the electric field-induced splitting of the resonance frequencies,

$$\nu_Q = \frac{1}{2}A\left(1+\frac{\eta^2}{3}\right)^{1/2}, \tag{3}$$

where

$$A = \frac{e^2Q}{h}V_{zz}, \tag{4}$$

where h is Planck's constant, V_{zz} the principal component of the diagonalized electric field gradient tensor, and η the asymmetry parameter (zero for Cu in $3R$-$CuAlO_2$). Q is the nuclear quadrupole moment.

The electric field gradient tensor, $\bar{\bar{V}}$, is calculated using the nonspherical part (in fact, the $\ell=2$ component) of the crystalline Hartree potential

$$V_{ij} = \frac{\partial^2 V_{H,\ell=2}}{\partial x_i\, \partial x_j}, \tag{5}$$

where the derivatives are evaluated at the site of the atomic nucleus. Denoting the eigenvalues of $\bar{\bar{V}}$ by V_{xx}, V_{yy}, and V_{zz} with $|V_{xx}| \le |V_{yy}| \le |V_{zz}|$, the electric field gradient per definition is equal to V_{zz} while the asymmetry parameter is

$$\eta = \frac{V_{xx}-V_{yy}}{V_{zz}}, \tag{6}$$

which lies in the range [0,1] (since $V_{xx}+V_{yy}+V_{zz}=0$).

We refer to V_{zz} as the EFG. The full potential of the QSGW is nonlocal but the EFG is derived from the Hartree potential, which is local. Thus, although we here use QSGW, the EFG is derived completely "as usual."[47]

From the NQR measurements by Abdullin *et al.*,[48] the magnitude of the EFG on Cu becomes 10.6×10^{21} V/m^2 (the experiment does not give the sign of the EFG). A straight LDA calculation gives -5×10^{21} V/m^2, i.e., only half the measured magnitude. One can obtain the correct value by the LDA+U approximation but in our scheme this requires a U_{eff} of about 13 eV, as can be seen from Fig. 12

The QSGW gives the correct value of the EFG at the equilibrium volume. Figure 13 shows the EFG as calculated for varying volume, using three different approaches, LDA, LDA plus a self-consistent down shift by 2.5 eV of the copper d states, and (for two volumes only) by means of the QSGW. It is seen that the simple method of applying the d downshift yields EFG values very close to those obtained by the QSGW.

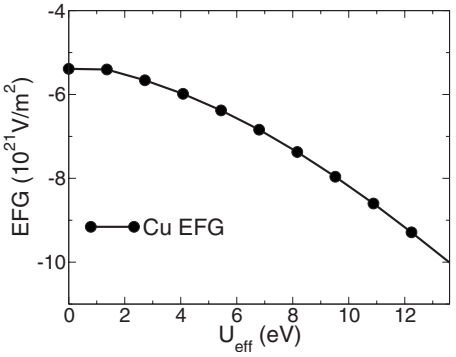

FIG. 12. $3R$-$CuAlO_2$: the electrical field gradient on Cu calculated by means of LDA+U as a function of U_{eff}.

V. GAP DEFORMATION POTENTIALS

Application of external pressure in optical experiments provides valuable data for a detailed analysis. The measurement of deformation potentials,

$$\alpha = dE_g/d\ln V \tag{7}$$

of gaps, E_g, and the pressure coefficients,

$$\gamma = dE_g/dP, \tag{8}$$

are essential in the assignment of the spectral features to the electronic structure. These quantities were calculated for $CuAlO_2$, using both QSGW and LDA approximations. Direct as well as indirect gaps were examined, see Table I. (It should be recalled, however, that the VBM in fact is not at a high-symmetry point, see Fig. 7 and Ref. 37.)

The pressure coefficients, γ, were obtained by dividing α by the value of the experimental[24] bulk modulus, 200 GPa. Although the LDA yields considerably smaller values of all gaps than QSGW, it is seen from Table I that both sets of calculations predict that, considering only states at the high-symmetry points, the indirect $\Gamma \rightarrow \Gamma$ gap is the lowest gap and that smallest direct gap is at L. This is in agreement with other calculations, for example, Refs. 17 and 23 (see also Sec. III). Note that we use a different[10] convention for labeling the high-symmetry points in the Brillouin zone than the one adapted by Pellicer-Porres *et al.*[23] Their point X corre-

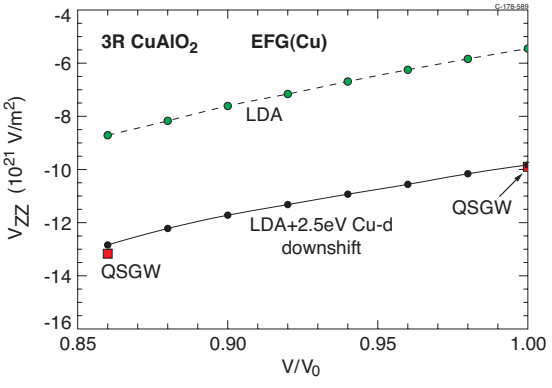

FIG. 13. (Color online) $3R$-$CuAlO_2$: the electrical field gradient calculated by means of LDA, QSGW, and LDA plus a self-consistent 2.5 eV downshift (see text) of the Cu $3d$ states.

TABLE I. Gaps, E_g (eV), and deformation potentials (α in eV) and pressure coefficients (γ in meV/GPa) direct band gaps at Γ, F, L, and Z and three indirect gaps, $F_{VB}\rightarrow\Gamma_{CB}$, $L_{VB}\rightarrow\Gamma_{CB}$, and $F_{VB}\rightarrow L_{CB}$ VB: highest valence-band state and CB: lowest conduction-band state. QSGW as well as LDA results are listed.

Gap	Γ→Γ	F→F	L→L	Z→Z	F→Γ	L→Γ	F→L
E_g QSGW	5.99	4.87	4.55	7.47	4.23	4.36	4.49
α	−4.9	2.6	2.7	−4.1	−3.2	−3.3	3.3
γ	24.5	−12.9	−13.6	20.4	16.0	16.3	−14.5
E_g LDA	2.90	2.93	2.66	4.28	1.95	2.03	2.57
α	−5.4	1.2	1.3	−4.2	−3.9	−4.0	1.4
γ	26.9	−6.1	−6.5	20.8	19.4	20.0	−7.2
γ [a], LDA			−6		16	16	

[a]Reference 23.

sponds to F here and their T is our Z point. We were, in our setup, not able to locate the point called P in Ref. 23 but we made a systematic search in the Brillouin zone and did not find a direct gap which is smaller than the one at L.

LDA and QSGW give significantly different results for the deformation potentials (and pressure coefficients) of the direct gaps at F and L. The LDA values are only around 50% of those obtained by QSGW. The analysis of the experimental absorption data in Ref. 23 showed that the pressure coefficient of the indirect absorption edge is 15 meV/GPa, in excellent agreement with the LDA calculations in Refs. 16 and 23 meV/GPa, also included in Table I, last line. A similar agreement is also found when comparing to our calculation, but best with the QSGW results, 16.0 and 16.3 meV/GPa for the F→Γ and L→Γ gaps, respectively. Our LDA values are somewhat larger than those in Ref. 23. Again, it should be recalled that the analysis of the optical absorption near the edge is complicated by the exciton (direct and indirect) states.

It is well established that $3R$-$CuAlO_2$ is an indirect-gap semiconductor at ambient pressure. But Table I shows that the smallest direct gap (at L) has a negative pressure coefficient, whereas the lowest indirect gap (F→Γ) has a positive γ value. From the QSGW values of the gaps and γ, i.e., using a linear variation in the gaps with pressure, we find that the two gaps become equal at ≈11 GPa. This does not imply, however, that the material is a direct-gap semiconductor at pressures above 11 GPa. The indirect F→L gap has also a negative pressure coefficient and it becomes the lowest indirect gap at ≈8 GPa, i.e., at a lower pressure than the 11 GPa, where the direct gap equals the F→Γ gap.

A similar behavior is found when the LDA approximation is used but instead of 11 and 7 GPa, the transition pressures would be ≈27 and 23 GPa. It has been found experimentally[24,25] that $CuAlO_2$ undergoes a structural transformation as the applied pressure exceeds 36 GPa. We calculated the gaps in $3R$-$CuAlO_2$ for a volume $V=0.86\times V_0$, where $P\approx 32$ GPa according to Fig. 2. Table II lists the gaps at this compressed volume (using the optimized structural parameters). According to the results in Table II the band structure still at this elevated pressure has an indirect gap, F→L. But it is only 0.06 (QSGW) to 0.08 eV (LDA) smaller than the direct gap at L.

Figure 14 shows the band structures as calculated (QSGW) for ambient pressure and when the 32 GPa hydrostatic pressure is applied. The figure shows how the band structure still at the high pressure has an indirect gap, although the L-L direct gap has decreased. The final state for indirect transitions changes from Γ to L. At both pressures we find the VBM state at the dot, marked in the figure. The highest F state is 84 meV below the VBM at zero pressure, whereas the corresponding energy difference is 72 meV in the compressed crystal. Since the shape of the relevant part of the upper valence band hardly changes upon application of 32 GPa pressure, we conclude that the calculated pressure coefficients for the indirect gaps in $3R$-$CuAlO_2$ are well represented by the calculations in Table I, even when the initial states are assumed to be at F and L, and not at the "true" VBM, the dots in Fig. 7. We checked this statement by calculating (using a small compression) the deformation potential of $F_{VB}\rightarrow$ VBM and find that it corresponds to a pressure coefficient $\gamma=1$ meV/GPa, when calculated in the QSGW approximation and 0 meV/GPa in LDA.

VI. SUMMARY AND CONCLUSION

Although copper aluminate has been studied extensively, both by theoretical and experimental methods, in the past, we

TABLE II. The same gaps, E_g (eV), as listed in Table I, but calculated for a hydrostatic compression to 86% of the equilibrium volume, $P\approx 32$ GPa.

Gap	Γ→Γ	F→F	L→L	Z→Z	F→Γ	L→Γ	F→L
E_g QSGW	6.87	4.53	4.18	8.15	4.82	4.88	4.12
E_g LDA	3.78	2.75	2.44	4.97	2.60	2.68	2.36

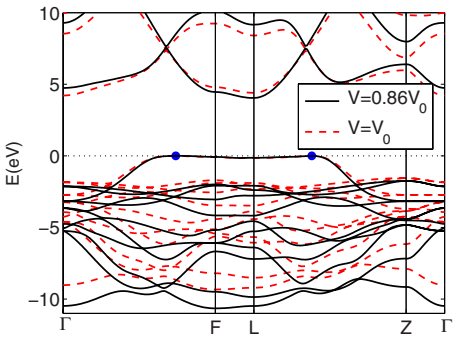

FIG. 14. (Color online) Comparison of the QS*GW* band structures calculated for $CuAlO_2$ at the equilibrium volume (V_0) (red dashed) and at the reduced volume, $0.86\times V_0$ (black full-line curves). The energy was set to zero at the VBM, indicated by the dot at a point on Γ-F. The two band plots are lined up to a common reference energy, their VBMs. Therefore the dot with k vector on the L-Z line represents two energies, −0.3 meV for $V=V_0$ and −0.4 meV for $V=0.86\times V_0$.

have chosen this material for a comparative study of three "band-structure methods." The reason for this is that $CuAlO_2$ is technologically very important and that it therefore may be particularly interesting to test various theoretical approaches for this material.

As expected, the formal one-electron band structure obtained from the Kohn-Sham LDA eigenvalues yields a band gap which is far too small. Further the Cu 3*d* states lie at too high energies. Both these errors are "typical LDA errors" when the LDA bands are compared to *optical* measurements. But the LDA bands are not, in principle, suited for excited-state calculations and it may therefore seem surprising that we in the past have been able to, even for semiconductors (by making simple corrections, "scissors operators" etc.), perform useful analyses of optical data from such band structures.

The LDA+U scheme introduces corrections for both LDA errors mentioned. The down shift of the Cu *d* states reduces the hybridization to the uppermost valence-band states and this leads to an increase in the band gaps. This effect is large in $CuAlO_2$ but a similar effect cannot be obtained in many other semiconductors, such as silicon (no high-lying narrow bands).

Although the LDA+U in $CuAlO_2$ affects the electrical field gradient, EFG, on Cu an effective U value which is much larger than the one used to adjust the gap must be applied in order to obtain a proper EFG value. The LDA yields an EFG value which is only half of the measured magnitude. In order to obtain this result we had to choose an effective U near 13 eV. On the other hand, the gap adjustment *and* the adjustment of the Cu 3*d* peak position to XPS spectra were made by choosing $U_{eff}=8.2$ eV. It is not surprising that the measured values of these two different quantities cannot be reproduced by LDA+U with the same value of U_{eff}; the EFG is a ground-state property, whereas XPS and optical-absorption measure excitations.

One way to calculate a quasiparticle band structure is to apply the *GW* approximation. In the *GW*-LDA one *GW* calculation is made on top of the LDA. We have here used the QS*GW* scheme in which the self-energy is iterated to self-consistency so that no errors are "inherited" from the LDA. The quasiparticle bands obtained in this way exhibit larger gaps, in fact somewhat too large as generally found for semiconductors. As mentioned, the gap will be reduced if vertex corrections are included and in $CuAlO_2$ the excitonic effects (e-h correlations) have been estimated to reduce the gap by ≈0.8 eV. It has also been stressed that electron-phonon gap-renormalization effects should be taken into account when theoretical and experimental gap values are compared. Further, the QS*GW* appears to improve the description of the electron correlation in the Cu *d* states. The EFG as calculated, for ambient pressure, in this scheme for $CuAlO_2$ agrees with experiment and it is very different from the value obtained within the LDA. Comparing QS*GW* and LDA calculations of EFGs for GaN has shown that in that case almost the same values were obtained by the two approximations. Although the Ga 3*d* are lying somewhat too high in LDA, they are, in contrast to the Cu 3*d*, so far from the upper valence bands that they only slightly affect the EFG.

Various effects of applying external pressure have been predicted. The *P*-*V* relation and the volume variation in the bulk modulus were derived from total (LDA) energies. For this purpose also the volume (pressure) variation in the structural parameters c/a and u was derived. The values obtained for ambient pressure agree very well with experiments and other calculations, for example, Ref. 12. To our knowledge there is no experimental information available about pressure effects on c/a and u. The predicted volume variation in the EFG also awaits experimental verification. For some of the band gaps we found surprisingly large differences between the deformation potentials as derived with the QS*GW* and LDA approximations. The pressure coefficient (QS*GW*) of the indirect absorption edge appears to agree extremely well with experiments. The QS*GW* and LDA values of the pressure coefficient of the lowest direct (L-L) gap differ by a factor of ≈2. A possibility to compare to a measured value of this quantity would therefore be very interesting. The present calculations predict, QS*GW* as well as LDA, that 3*R*-$CuAlO_2$ is an indirect-gap semiconductor over its entire stability pressure range, 0–36 GPa, but that the final state of the smallest (indirect) gap shifts from the Γ point at ambient pressure to L at higher pressures, P above ≈8 GPa (QS*GW*).

ACKNOWLEDGMENTS

This work was supported by the Danish Agency for Science Technology and Innovation under Grant No. 272-06-0432. The calculations were carried out at the Centre for Scientific Computing in Aarhus, financed by the Danish Centre for Scientific Computing and the Faculty of Natural Science, Aarhus University.

[1] C. Friedel, Acad. Sci., Paris, C. R. **77**, 211 (1873).
[2] F. A. Benko and F. P. Koffyberg, J. Phys. Chem. Solids **45**, 57 (1984).
[3] H. Kawazoe, M. Yasukawa, H. Hyodo, M. Kurita, H. Yanagi, and H. Hosono, Nature (London) **389**, 939 (1997).
[4] H. Kizaki, K. Sato, A. Yanase, and H. Katayama-Yoshida, Jpn. J. Appl. Phys., Part 2 **44**, L1187 (2005).
[5] H. Katayama-Yoshida, K. Sato, H. Kizaki, H. Funashima, I. Hamada, T. Fukushima, V. A. Dinh, and M. Toyoda, Appl. Phys. A: Mater. Sci. Process. **89**, 19 (2007).
[6] A. N. Banerjee, R. Maity, P. K. Ghosh, and K. K. Chattopadhyay, Thin Solid Films **474**, 261 (2005).
[7] Y.-C. Liou and U.-R. Lee, J. Alloys Compd. **467**, 496 (2009).
[8] H. Yanagi, S.-i. Inoue, K. Ueda, H. Kawazoe, H. Hosono, and N. Hamada, J. Appl. Phys. **88**, 4159 (2000).
[9] D. J. Aston, D. J. Payne, A. J. H. Green, R. G. Egdell, D. S. L. Law, J. Guo, P. A. Glans, T. Learmonth, and K. E. Smith, Phys. Rev. B **72**, 195115 (2005).
[10] C. J. Bradley and A. P. Cracknell, *The Mathematical Theory of Symmetry in Solids* (Clarendon, Oxford, 1972).
[11] B. J. Ingram, T. O. Mason, R. Asahi, K. T. Park, and A. J. Freeman, Phys. Rev. B **64**, 155114 (2001).
[12] X. Nie, S.-H. Wei, and S. B. Zhang, Phys. Rev. Lett. **88**, 066405 (2002).
[13] V. I. Anisimov, J. Zaanen, and O. K. Andersen, Phys. Rev. B **44**, 943 (1991).
[14] V. I. Anisimov, I. V. Solovyev, M. A. Korotin, M. T. Czyżyk, and G. A. Sawatzky, Phys. Rev. B **48**, 16929 (1993).
[15] V. I. Anisimov, F. Aryasetiawan, and A. I. Lichtenstein, J. Phys.: Condens. Matter **9**, 767 (1997).
[16] L. J. Sham and T. M. Rice, Phys. Rev. **144**, 708 (1966).
[17] R. Laskowski, N. E. Christensen, P. Blaha, and B. Palanivel, Phys. Rev. B **79**, 165209 (2009).
[18] M. van Schilfgaarde, T. Kotani, and S. V. Faleev, Phys. Rev. Lett. **96**, 226402 (2006).
[19] T. Kotani, M. van Schilfgaarde, and S. V. Faleev, Phys. Rev. B **76**, 165106 (2007).
[20] M. van Schilfgaarde, T. Kotani, and S. V. Faleev, Phys. Rev. B **74**, 245125 (2006).
[21] S. V. Faleev, M. van Schilfgaarde, and T. Kotani, Phys. Rev. Lett. **93**, 126406 (2004).
[22] V. Jayalakshmi, R. Murugan, and B. Palinivel, J. Alloys Compd. **388**, 19 (2004).
[23] J. Pellicer-Porres, A. Segura, A. S. Gilliland, A. Muñoz, P. Rodriguez-Hernandez, D. Kim, M. S. Lee, and T. Y. Kim, Appl. Phys. Lett. **88**, 181904 (2006).
[24] J. Pellicer-Porres, D. Martinez-Garcia, A. Segura, P. Rodriguez-Hernandez, A. Muñoz, J. C. Chervin, N. Garro, and D. Kim, Phys. Rev. B **74**, 184301 (2006).
[25] P. Rodriguez-Hernández, A. Muñoz, J. Pellicer-Porres, D. Martinez-García, A. Segura, N. Garro, J. C. Chervin, and D. Kim, Phys. Status Solidi B **244**, 342 (2007).
[26] O. K. Andersen, Phys. Rev. B **12**, 3060 (1975).
[27] A. Buljan, P. Alemany, and E. Ruiz, J. Phys. Chem. B **103**, 8060 (1999).
[28] N. E. Christensen, in *High Pressure in Semiconductor Physics I*, Semiconductors and Semimetals Vol. 54, edited by T. Suski, W. Paul, R. K. Willardson, and E. R. Weber (Academic, New York, 1998), p. 49.
[29] N. E. Christensen, Phys. Rev. B **30**, 5753 (1984).
[30] I. Gorczyca, J. Plesiewicz, L. Dmowski, T. Suski, N. E. Christensen, A. Svane, C. S. Gallinat, G. Koblmueller, and J. S. Speck, J. Appl. Phys. **104**, 013704 (2008).
[31] L. Hedin and S. Lundqvist, in *Solid State Physics*, edited by H. Ehrenreich, F. Seitz, and D. Turnbull (Academic, New York, 1969), Vol. 23, p. 1.
[32] A. N. Chantis, M. van Schilfgaarde, and T. Kotani, Phys. Rev. Lett. **96**, 086405 (2006).
[33] A. N. Chantis, M. van Schilfgaarde, and T. Kotani, Phys. Rev. B **76**, 165126 (2007).
[34] A. N. Chantis, M. Cardona, N. E. Christensen, D. L. Smith, M. van Schilfgaarde, T. Kotani, A. Svane, and R. C. Albers, Phys. Rev. B **78**, 075208 (2008).
[35] P. Modak, A. Svane, N. E. Christensen, T. Kotani, and M. van Schilfgaarde, Phys. Rev. B **79**, 153203 (2009).
[36] M. Methfessel, M. van Schilfgaarde, and R. A. Casali, *Lecture Notes in Physics* (Springer-Verlag, Berlin, 2000), Vol. 535.
[37] The VBM is not at F. There are points along Γ-F and L-Z, for example, with slightly higher valence-state energies, as also found in Ref. 12.
[38] M. Shishkin, M. Marsman, and G. Kresse, Phys. Rev. Lett. **99**, 246403 (2007).
[39] R. Laskowski and N. E. Christensen, Phys. Rev. B **74**, 075203 (2006).
[40] R. Laskowski and N. E. Christensen, Phys. Rev. B **73**, 045201 (2006).
[41] R. Laskowski, N. E. Christensen, G. Santi, and C. Ambrosch-Draxl, Phys. Rev. B **72**, 035204 (2005).
[42] Y. P. Varshni, Physica (Amsterdam) **34**, 149 (1967).
[43] M. Cardona, T. A. Meyer, and M. L. W. Thewalt, Phys. Rev. Lett. **92**, 196403 (2004).
[44] M. Cardona and M. L. W. Thewalt, Rev. Mod. Phys. **77**, 1173 (2005).
[45] N. E. Christensen, D. L. Novikov, R. E. Alonso, and C. O. Rodriguez, Phys. Status Solidi B **211**, 5 (1999).
[46] N. E. Christensen and M. Methfessel, Phys. Rev. B **48**, 5797 (1993).
[47] A. Svane, N. E. Christensen, C. O. Rodriguez, and M. Methfessel, Phys. Rev. B **55**, 12572 (1997).
[48] R. S. Abdullin, V. P. Kal'chev, and I. N. Pen'kov, Phys. Chem. Miner. **14**, 258 (1987).